Development of a prototype snow albedo algorithm for the NASA MODIS Instrument

ANDREW G. KLEIN,[1] DOROTHY K. HALL,[2] AND ANNE W. NOLIN[3]

ABSTRACT

A prototype snow albedo algorithm has been developed for the Moderate Resolution Imaging Spectroradiometer (MODIS). The prototype algorithm is designed to enable daily snow albedo determination for cloud free areas mapped as snow by the MODIS snow-mapping algorithm. The bidirectional reflectance distribution function (BRDF) of snow is modeled using a discrete ordinates radiative transfer model to allow for the correction of anisotropic scattering effects over non-forested surfaces. For forested areas, a simple Lambertian scattering model is assumed. The effects of illumination and viewing geometries are also considered in the albedo determination. Initial prototyping efforts were accomplished using MODIS Airborne Simulator (MAS) data acquired over Wisconsin and New York during January and February 1997. Despite limited concurrent field observations for validation, the prototype algorithm's performance appears reasonable in the visible part of the spectrum. However, correction for anisotropic scattering effects in the shortwave infrared region of the spectrum remains problematic.

Key words: remote sensing, albedo, snow

INTRODUCTION

Snow is one of the Earth's brightest natural surfaces with the albedo of newly fallen snow often exceeding 80%. Small variations in snow albedo can have a profound influence on surface energy fluxes as has recently been demonstrated for the Greenland ice sheet by Nolin and Stroeve (1997). In addition, snow cover is significant in terms of its areal extent. It influences not only local and regional scale processes but also affects the Earth's global heat budget (Barnett *et al.*, 1989).

Changes in the albedo of a snowpack are driven by surface grain size, the concentration of light absorbing particulates (dust and soot) and, for thin snow, by snow depth. Hence, snow albedo varies considerably spatially (e.g. Knap *et al.*, 1999; Knap and Oerlemans, 1996; Stroeve *et al.*, 1997) and thus ground based measurements of snow albedo may be unrepresentative of larger areas (Greuell and de Wildt, 1999). The albedo of a snow pack also changes dramatically over time. Deposition of new snow can cause a nearly instantaneous increase in albedo and the onset of

[1] Department of Geography, MS 3147, Texas A&M University, College Station, Texas 77843-3147
tel: 979 845 5219, fax: 979 862 4487, email: klein@geog.tamu.edu

[2] Hydrological Sciences Branch, Code 974, NASA/Goddard Space Flight Center, Greenbelt, MD 20771

[3] [3]Cooperative Institute for Research in Environmental Sciences, University of Colorado, Boulder, CO 80309-0449

snowmelt and its ensuing grain growth can cause snow albedo to decrease substantially in a matter of hours. In several environmental settings the albedo of snowpacks has been observed to decrease from 80% or more, immediately after a snowfall to 20% - 40% in two weeks or less (O'Neill and Gray, 1973; Winther, 1993b).

Satellites provide a means to monitor both spatial and temporal variability in snow albedo over large areas. A large body of work has been undertaken to utilize the ability of satellites to map the albedo of snow and glaciers (Hall *et al.*, 1989; Knap and Oerlemans, 1996; Reijmer *et al.*, 1999; Robinson and Kukla, 1985; Stroeve *et al.*, 1997; Winther, 1993a) as well as sea ice (De Abreau *et al.*, 1994; Lindsey and Rothrock, 1994). The research described here builds on this previous work to develop a prototype clear-sky albedo algorithm for use with the recently launched NASA Moderate Resolution Imaging Spectroradiometer (MODIS). This algorithm will be used to determine the albedo of surfaces mapped as snow by the MODIS snow-mapping algorithm (for complete algorithm descriptions see Hall *et al.*, 1995; Hall *et al.*, 1998; Klein *et al.*, 1998). As additional MODIS data becomes available for validation, the algorithm may be extended to areas identified as sea ice by the MODIS sea ice algorithm (Riggs *et al.*, 1999). The results of the prototyping efforts presented here were conducted using MODIS Airborne Simulator (MAS) imagery acquired over New York and Wisconsin during February 1997 as MODIS data was not be available on a regular basis until the summer of 2000.

THEORETICAL BACKGROUND

Albedo (a) is the dimensionless ratio of reflected to incident irradiance measured in a surface-parallel plane. It is also termed the directional-hemispherical reflectance as the incident irradiance is considered a directional collimated beam and the reflected radiance is integrated over the upward hemisphere. In addition, the albedo of most interest in energy balance studies and that typically measured in the field by pyranometers is a broadband albedo. However, MODIS measures the Top-of-Atmosphere (TOA) radiances received from the surface in a set of relatively narrow spectral intervals (bands). Creation of a broadband albedo estimate from the MODIS TOA radiances requires that a set of adjustments be made. These adjustments include (1) calibration of the satellite sensors, (2) correction for atmospheric effects, (3) correction for anisotropic reflection at the surface and (4) calculation of a spectrally-integrated albedo (Greuell and de Wildt, 1999). To this list could be added a correction for slope induced variations in incident radiation (Proy *et al.*, 1989). Additional information about the prototype algorithm can be found in Klein and Hall (1999).

Sensor calibration and atmospheric correction

Adequate calibration of the satellite sensor is less of an issue with MODIS than with other instruments as MODIS data provided to the science community will be extensively calibrated (Barbieri *et al.*, 1997). While MODIS data is well calibrated, the TOA radiances measured by MODIS are a function of the physical properties of the snow surface and atmospheric conditions at the time of image acquisition. Thus, the prototype algorithm developed here derives an albedo affected by both surface and atmospheric conditions.

Cloud detection and correction of the TOA radiances for atmospheric affects will be accomplished using existing MODIS products. Snow albedo will only be determined for areas identified as cloud-free by the MODIS cloud mask (Ackerman *et al.*, 1997). Atmospheric correction will be accomplished via the MODIS land surface reflectance product (Vermote and Vermeulen, 1999). While a detailed description of the potential problems with the MODIS atmospheric correction over snow and ice is beyond the scope of this paper, atmospheric corrections over snow remain a challenge. Over bright snow surfaces, aerosols have a darkening effect. Depending on aerosol type and optical depth, they can alter TOA reflectances in the visible wavelengths by as much as 20% (Nolin and Stroeve, 1999). Atmospheric corrections for the MAS prototyping efforts presented here employed the 6S atmospheric simulation code, which forms the foundation for the actual MODIS surface reflection algorithm (Vermote *et al.*, 1997). Correction for anisotropic reflection

After accounting for instrument calibrations and atmospheric affects, the next step in creating an albedo estimate is correcting for the anisotropic reflection of snow. Failure to do so can lead to errors in estimated albedo (Stroeve *et al.*, 1997). Because both MODIS and MAS sample only a small angular portion of the total energy reflected from the surface, this angular measurement

must be converted to a hemispherical quantity. If the reflection from the surface were isotropic, a single measurement would be representative of all angles. However, like most earth surfaces, snow is a non-Lambertian reflector. In fact, snow is strongly forward scattering. Because the energy reflected from a snow surface is unevenly distributed among reflection angles, knowledge of the actual angular distribution of this reflected energy - termed the bidirectional reflectance distribution function or BRDF (Nicodemus *et al.*, 1977) - is needed to correctly account for anisotropic scattering effects.

In snow albedo research correction for anisotropic scattering effects has traditionally been accomplished by normalizing the BRDF by the spectral albedo (the albedo within a narrow spectral interval) to create what is termed an anisotropic response function (ARF or *f*). The ARF is used as an adjustment factor for the satellite measurements in each spectral band. Values of $f > 1$ indicate that the reflectance observed at a particular combination of solar zenith angle, sensor zenith angle and relative azimuth between the sensor and the sun is greater than the spectral directional hemispherical albedo. Values of $f < 1$ indicate the observed reflectance is less than the spectral directional hemispherical albedo. If the complete BRDF or ARF is known for each MODIS band then it is possible to derive a spectral albedo measurement from a single satellite-derived measurement.

To date, BRDF or ARF functions for snow surfaces have been determined through two means. The first approach is to measure BRDF directly from field or satellite observations whereas the second method employs radiative transfer models to simulate the BRDF. Over the past several decades numerous bi-directional reflectance measurements have been made of snow and ice surfaces (e.g. Greuell and de Wildt, 1999; Knap *et al.*, 1999; Leshkevich *et al.*, 1990; Steffen, 1996). The use of empirically derived anisotropic reflectance factors for determining sea ice albedo has been accomplished by De Abreau *et al.* (1994) and Lindsey and Rothrock (1994) using correction factors developed from ERBE data (Taylor and Stowe, 1984). However, the current suite of measurements neither covers a large enough set of conditions nor suitably matches the MODIS bandpasses to be useful in developing a generalized anisotropic reflectance correction for the MODIS instrument.

Fortunately, snow is a particulate medium and radiative transfer models developed for atmospheric research can be adapted to snow modeling (Nolin and Liang, in press). Recently, several investigators (Fily *et al.*, 1997; Nolin and Stroeve, 1997; Stroeve *et al.*, 1997) have demonstrated the potential for using a Discrete-Ordinates Radiative Transfer model (Stamnes *et al.*, 1988) to model snow BRDF. DISORT is appropriate for modeling multiple scattering in particulate media and calculates the angular distribution of reflected radiation.

In the algorithm prototyping efforts, DISORT was used to construct a look-up table of ARF for the employed MAS bands. Values of ARF were computed for a wide range of solar and satellite zenith and azimuths as well as for varying ratios of direct to diffuse irradiance. The optical properties needed for the DISORT model include snowpack optical thickness, single scattering albedo, an asymmetry parameter or a description of the scattering phase function. These parameters can be calculated using Mie theory using the refractive indices for ice and assuming an optically equivalent grain size, which in this work was taken to be 250 μm. Examples of the DISORT model output are shown in **Figure 1**.

The anisotropic correction developed using DISORT is only applicable in areas where snow is the dominant surface in a MODIS pixel. However, as much of the seasonally snow-covered area of the world is forested this is often not the case. For instance, in North America approximately 40% of the area north of the continental snow line is covered by forests (Hall *et al.*, in press; Klein *et al.*, 1998). Currently measurements of the BRDF of snow-covered forests are lacking and no applicable model of the BRDF of a snow-covered canopy currently exists. Thus in the current prototype, the ARF correction is only applied to non-forested areas whereas forests are assumed lambertian reflectors.

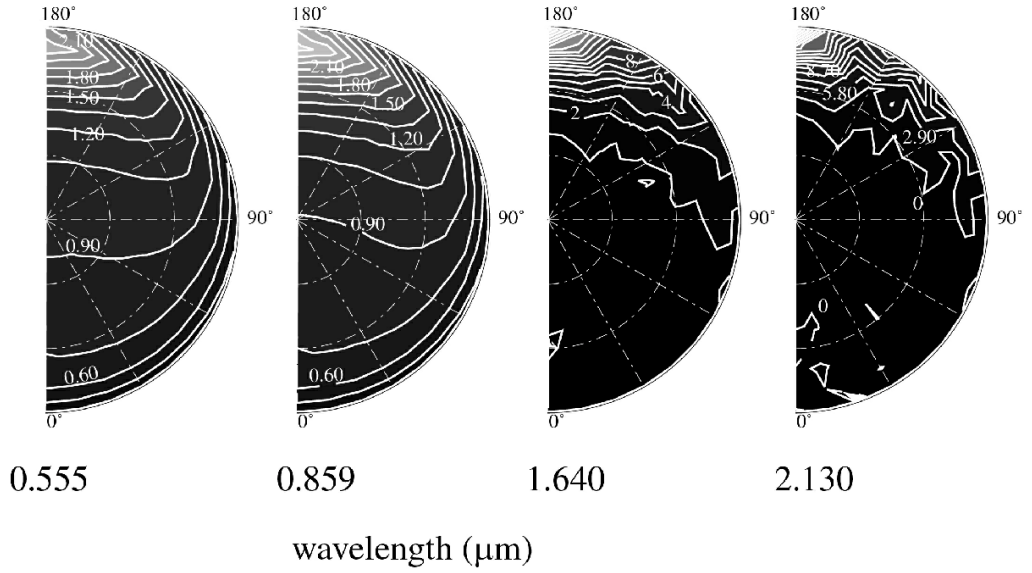

Figure 1. Anisotropic response function created from DISORT at four of the MAS wavelengths. These simulations consider only a direct beam (no diffuse irradiance), a solar zenith angle of 60°, and an optically equivalent grainsize of 250 μm. The distance from the origin indicates solar zenith angle while the direction indicates the relative azimuth between the sensor and the satellite (at 180° the sensor faces into the sun)

Calculation of a spectrally-integrated albedo

After correcting for anistropic scattering effects, a spectral albedo for each of the MAS bands can be computed. However, for most studies, a spectrally-integrated albedo, not a spectral albedo within satellite-specific bands, is of most interest. However, differences between the MODIS and MAS bands (discussed below) precluded the development of a narrow-to-broadband conversion using MAS data. However, a generalized approach for converting MODIS spectral albedo measurements to broad-band albedos has been formulated for MODIS and can be adapted use in a snow albedo algorithm. Using 100+ spectra, Liang *et al.* (1998) found that a linear combination of the seven MODIS land bands can predict the total shortwave albedo very accurately. The coefficients provide three albedo measures of broadband albedos: one in the visible (0.4-0.7 μm), a second in the near-IR (0.7-5.0 μm), and a third in the shortwave (0.25-5.0 μm) wavelengths.

MODIS AND THE MODIS AIRBORNE SIMULATOR

Launched aboard the Terra satellite on December 18th, 1999, MODIS is especially well suited for observation of the Earth's snow and ice covered regions as it images high latitudes on a daily basis. Snow albedo estimates will be made using MODIS bands 1 to 7 which lie in the 0.4 to 2.5 μm wavelength region and that are designed specifically for land-surface studies. While the utilized MODIS bands have spatial resolutions of 250 m (bands 1 and 2) or 500 m (bands 3 through 7), the albedo product will have a resolution of 1 km due to limitations in resolution of the some of the ancillary inputs.

As it was necessary to develop the initial snow albedo prototype prior to the availability of MODIS data, algorithm development was undertaken using data collected by the MAS. The MAS is a 50-band airborne scanning spectroradiometer flown aboard a NASA ER-2 high-altitude research aircraft. At a nominal flight altitude of 20 km, the MAS achieves a spatial resolution of 50 m. The MAS does have some limitations as a MODIS simulator. Only five of the seven MODIS land bands (1, 2, 4, 6, and 7) have MAS equivalents (2, 7, 1, 10, and 20). Because the MAS band passes are not identical to MODIS it was impractical to use MAS data to develop a narrow-to-broadband conversion. Nevertheless, prior to the launch of MODIS, the MAS was the

best instrument with which to develop a prototype MODIS snow albedo algorithm. King *et al.* (1996) provide a complete description of the MAS instrument.

STUDY SITES

The prototype algorithm was developed using a series of MAS images (**Table 1**) acquired in late January and February, 1997 over Madison, Wisconsin, and near Oneonta, New York, during the Winter Cloud Experiment (WINCE). The Madison site was selected because of the numerous images acquired over the city and because field measurements of spectral albedo were made on Lake Mendota. The Oneonta was used to assess the performance of the slope correction that was difficult given the relatively flat terrain in Wisconsin.

Table 1. Basic information concerning the MAS images used in the study.

MAS ID	Date	Local	Visibility	Sky Cover	Aircraft	Solar Position	
			miles		*km*	*azimuth*	*zenith*
97-041-10	1/28/97	13:03	10	Clear	19.30	195	63
97-043-03	1/30/97	11:57	6	Overcast	19.41	178	61
97-043-05	1/30/97	12:32	6	Overcast	19.37	188	61
97-044-20	2/2/97	14:42	10	Few	20.24	221	70
97-045-16	2/6/97	14:00	10	Broken	19.76	237	78
97-046-25	2/8/97	14:26	10	Clear	20.00	216	66
97-046-27	2/8/97	14:35	10	Clear	19.99	218	67
*97-047-06	2/9/97	12:28	10	Clear	18.31	183	57
97-049-13	2/12/97	13:46	10	Clear	19.65	207	61
97-049-14	2/12/97	13:55	10	Clear	19.73	209	62
97-050-02	2/13/97	10:41	10	Clear	18.81	156	60

*Oneonta, New York

ALGORITHM DEVELOPMENT

The philosophical approach used to construct the snow albedo prototype embodied two concepts. The first was to limit development time by building upon recent work on satellite determination of snow albedo. In particular, the work of Nolin and Stroeve (1997) and Stroeve *et al.* (1997) provided a solid basis for the construction of a global snow albedo algorithm, especially in the area of correction for anisotropic scattering. Secondly, extensive use was made of existing MODIS products to minimize the computation load. While the major theoretical issues have been discussed above a brief discussion of some implementation details pertaining to algorithm inputs and MAS specific processing are warranted and are discussed briefly below.

MODIS inputs

The MODIS snow albedo algorithm is not designed to be stand-alone; instead it will take full advantage of existing MODIS products. As stated earlier, albedo will only be determined for areas identified as cloud-free by the MODIS cloud mask (Ackerman *et al.*, 1997) and as snow by the MODIS snow mapping algorithm (Hall *et al.*, 1998). Atmospheric correction will be accomplished via the MODIS land surface reflectance product (Vermote and Vermeulen, 1999). In the prototyping efforts, MAS versions of the cloud mask and snow classification algorithms were used as surrogates for the required inputs and 6S was used for atmospheric correction. In the 6S simulations, a typical mid-latitude winter atmospheric profile was assumed and visibility recorded at local airports near the time of each MAS overflight was used as a measure of aerosol optical depth.

Slope and aspect

Ancillary non-MODIS products are also required inputs into the albedo algorithm. As snow cover is prevalent in mountainous areas, correction of the surface reflectance for topographic

effects is necessary (e.g., Dozier and Marks, 1987; Proy *et al.*, 1989). Currently, the algorithm corrects for the orientation of the surface relative to the sun, but ignores effects of radiation reflected from and shadows cast by adjacent topography.

For MODIS, the Global 30 Arcsecond (GTOPO30) digital elevation model (DEM) available from the United States Geological Survey (USGS) will be used for the topographic corrections. The resolution of GTOPO30 is approximately 1 km, which will necessitate producing the snow albedo product at 1 km as opposed to the 500 m resolution of the snow cover products. However, the 50 m resolution of the MAS required a higher resolution DEM. For the prototyping efforts 30 m DEMs, also available from the USGS were complied for each area and resampled to the 50 m MAS resolution. The slope and aspect of each 50 m pixel was then determined using a best-fit plane to a moving 3 x 3 pixel window after correcting for some minor seams between individual DEMs.

Land use/land cover

Land use/land cover (LULC) information was used to determine whether an isotropic or anisotropic reflectance model should be employed. Initially, the MODIS algorithm will utilize the 1 km Global Landcover Characterization Database available from the USGS EROS data center, but eventually the MODIS Landcover/Landcover Change product (Strahler *et al.*, 1999) will be used.

Like the DEM, higher resolution LULC data is required for use with the MAS images. For the New York State site, the 1:250,000 LULC data set for the United States was used (DOI and USGS, 1986). For Wisconsin, a comprehensive land cover data set derivived from Landsat Thematic Mapper images and that adheres to National Gap Analysis Program protocols was used (http://www.dnr.state.wi.us/org/at/et/geo/data/wlc.htm). In both cases the original LULC maps were resampled to 50 m and the numerous original landcover classes were reclassified into a binary map (forested/non-forested).

MAS specific processing

Several steps were required to produce the necessary inputs for the prototype snow albedo algorithm from the original MAS data (**Table 1**). The radiance values of the five MAS bands with MODIS equivalents (1,2, 7, 10, and 20) were converted to reflectance units prior to atmospheric correction using standard methods (Gumley *et al.*, 1994). The MAS resulting reflectances, as well as the cloud mask and snow map produced from the original MAS images, were projected into a Universal Transverse Mercator (UTM) projection with 50 m resolution using nearest neighbor resampling. The ancillary datasets were projected into the same the UTM projection.

RESULTS AND DISCUSSION

The developed prototype was successfully run on a series of 10 MAS images from the Wisconsin site and 1 from the New York State site. Example atmospherically corrected and spectral albedo images from three dates over the Wisconsin site from MAS bands 1 and 10 are shown in **Figures 2** and **3**, respectively. These prototyping efforts demonstrated the feasibility of the proposed approach and enabled the implementation of the approach in a manner easily adaptable to actual MODIS data. In addition, some preliminary algorithm validation has been possible, but the extent of validation has been limited by problems with MAS itself and the paucity of concurrent MAS and field observations. However, the prototyping efforts have highlighted a number of potential problems that must be addressed in future versions of the algorithm that will apply to MODIS data.

Part of the difficulty in developing a snow albedo algorithm lies with the performance of the MAS itself. **Figure 4a** illustrates a series of field spectra taken on Lake Mendota on January 28th and atmospherically-corrected MAS reflectances averaged over a 500 x 500 meter area on the lake to simulate a single 500 m MODIS pixel (see **Figure 2** for sampling locations). While the atmospherically corrected MAS reflectances are not directly comparable to the field observations,

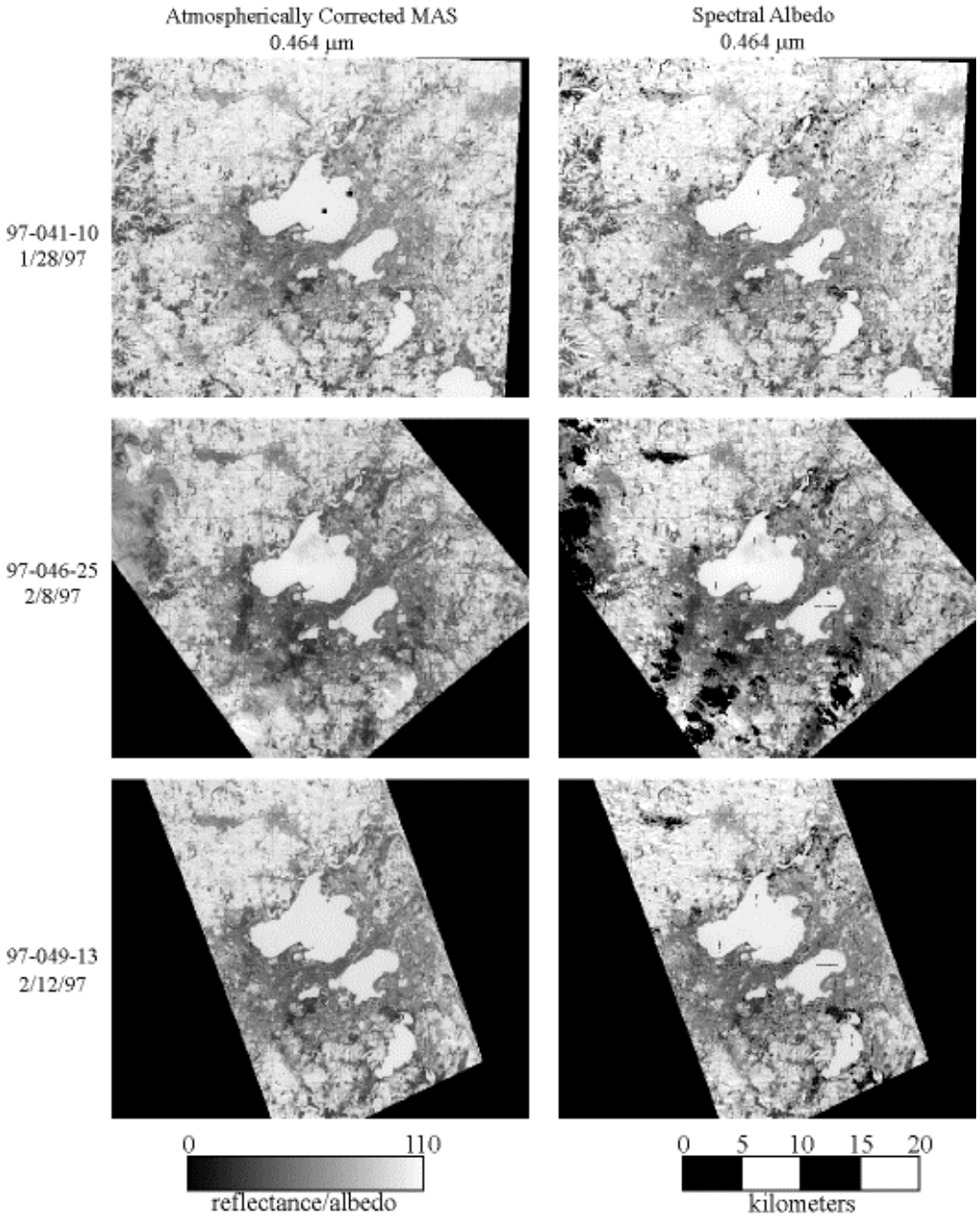

Figure 2. Atmospherically-corrected and spectral albedo images at 0.464 µm (MAS band 1). Lake Mendota is the largest lake in the image. The two black boxes in the upper-left image represent MODIS 500 meter pixels from which spectra were extracted. Black pixels in the spectral albedo image represent pixels for which the algorithm was not run due to clouds or lack of snow cover.

the atmospheric correction appears to have resulted in higher than actual reflectances in the visible portions of the spectrum. Because the production algorithm will use the MODIS land surface corrections, further refinement of the atmospheric correction was not attempted, but the results highlight the potential for problems with the atmospheric correction and clearly demonstrate the need for validation of the MODIS atmospheric correction algorithm over snow. Also evident in **Figure 4a** are highly elevated reflectances in the near infrared (MAS band 7). These elevated reflectances are due to problematic MAS radiances and not to the atmospheric correction. However, the cause of the problem responsible for the elevated reflectances is unknown. Compared to field observations, reflectances in MAS bands 10 and 20 are also slightly elevated.

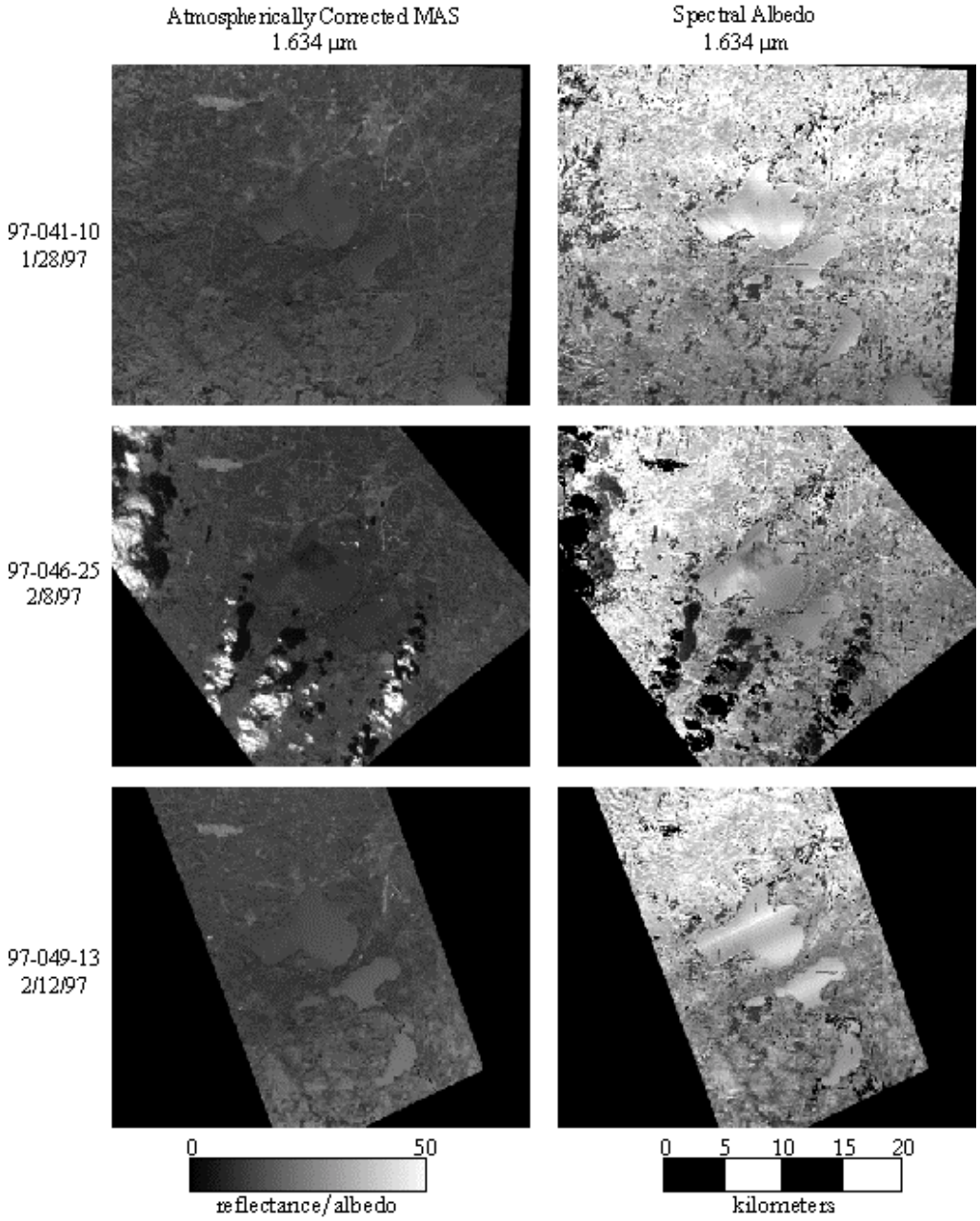

Figure 3. Atmospherically-corrected and spectral albedo images at 1.634 μm (MAS band 10).

The in-band spectral radiances from the five MAS bandpasses are shown in **Figure 4b**. Because Lake Mendota was typically imaged in a near nadir view (between 0.5° and 16.5° off-nadir), where the ARF of snow is slightly less than 1.0, the spectral albedos are higher than the atmospherically corrected reflectances. In particular, the spectral albedo in MAS bands 10 and 20 typically exceeded field measurements by 10-25%.

Both the spectral albedo images and comparisons with ground-based spectral measurements highlight a problem with the current prototype algorithm - the anisotropic correction in the bands centered at 1.6 μm and 2.1 μm. The current prototype simply performs better in the visible than shortwave-infrared portion of the spectrum. The problem is traceable to the DISORT model. While the modeled ARF appear to be reasonable in the visible and near-IR portions of the spectrum as can be seen in **Figure 1**, they appear suspect in the shortwave IR (1.6 and 2.1 μm bands). A different approach for generation of adequate ARF look-up tables for the shortwave MODIS bands may well be necessary.

Compared with ground-based measurements, DISORT tends to overestimate the strength of the forward scattering peak (Nolin and Stroeve, 1999) in the near-infrared wavelengths and is also sensitive to the accuracy of the solar and satellite zenith and azimuth angle determinations. Thus, the anistropic correction is not as robust as in the visible wavelengths. These factors cause the ARF for MAS bands 10 and 20 to vary much more over the study area than in for the visible bands (**Figure 5**), particularly the sensor begins to look south toward the sun. In turn, these variations in the ARF cause variations in the retrieved spectral albedo across the scene (**Figure 3**).

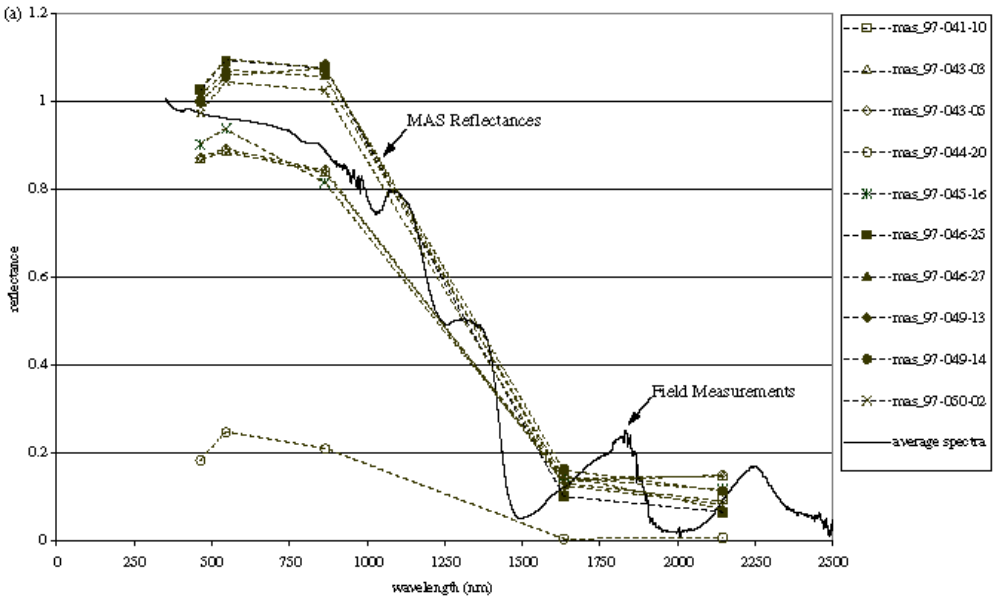

Figure 4a. MAS atmospherically-corrected surface reflectances averaged over a 500 x 500 meter area on Lake Mendota. Shown in both panels is the average of five field spectra collected on January 28th on the south-central portion of Lake Mendota. Atmospheric conditions at the time of the field spectra were collected were clear with a few high/thin cirrus clouds on the horizon and air temperature was -20° C. Snow depth was 10 cm and the snow pack was composed of hexagonal crystals with radii of 100-150 microns with some sintering of surface crystals. The field data were calibrated using the calibration coefficients developed for the Spectralon target by Alex Goetz (University of Colorado-Boulder).

However, in determining a broadband albedo, problems with bidirectional effects in the shortwave-infrared bands are somewhat mitigated by the fact that approximately 70% of the total exoatmospheric solar irradiance occurs at wavelengths shorter than 1 μm. As demonstrated by Stroeve *et al.* (1997) with AVHRR channels 1 and 2 and as proposed by Greuell and de Wildt (1999) for Landsat Thematic Mapper bands 1 to 4, it may be possible to construct an accurate broadband snow albedo estimate using the DISORT model/look up table approach with only a few MODIS visible and near infrared channels.

Additionally, the algorithm prototyping efforts clearly demonstrate the need for a slope correction. Without a slope correction, retrieved spectral albedos show a clear topographic signal with large differences in retrieved albedo occurring between slopes of different exposures. After correcting for topographic effects, the spectral albedo of slopes with different orientations is much less and albedo differences caused by other factors, such as differences between coniferous and deciduous canopies become much more apparent.

The algorithm prototyping efforts have also demonstrated the need for a daily snow albedo product given the large changes in the albedo of these surfaces over short time periods. The current MODIS land surface albedo algorithm (Lucht *et al.*, 2000; Wanner *et al.*, 1997) uses a 16 day temporal composite of MODIS and MISR (Multiangle Imaging Spectroradiometer) observations. These multiple observations are then fitted to one of a number of semi-empirical BRDF models, which are then integrated to determine two measures of surface albedo. One of these measures represents the irradiance under direct-beam irradiance and the other under completely diffuse irradiance (assuming isotropic diffuse irradiance). These albedos have an advantage over the albedo produced by the algorithm proposed here in that they measure the intrinsic albedo of the land surface, e.g. decoupled from the atmosphere. While this approach has advantages for many land covers by providing observations of seasonal changes in BRDF and albedo, it is poorly suited for snow studies. Many snow-covered regions are perpetually cloud-covered and, given the rapidity of change in the albedo of snow-covered surfaces, a 16-day composite albedo may not be representative of either the mean albedo nor its temporal variability.

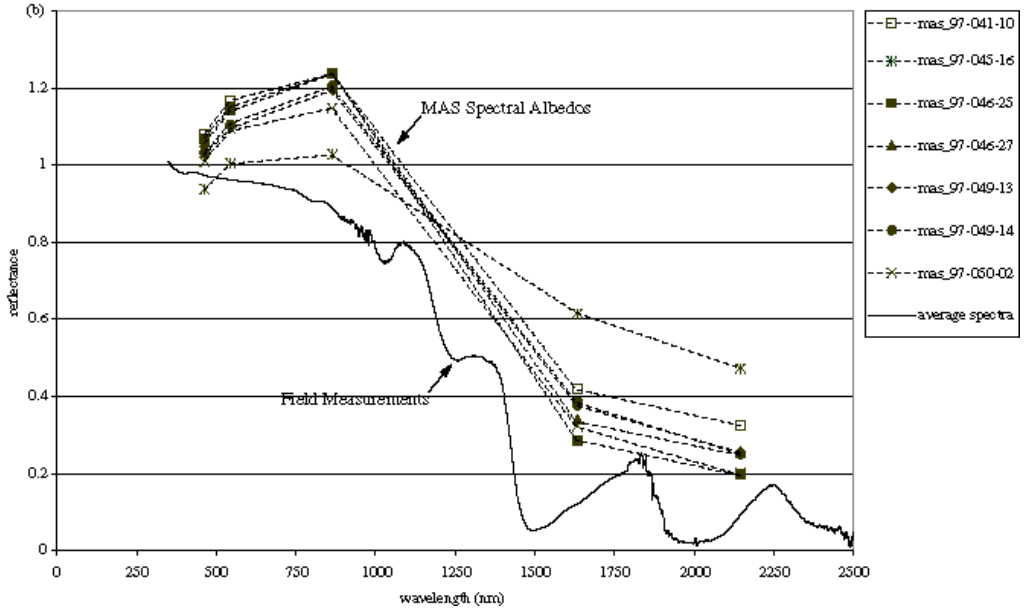

Figure 4b. Similar to 4a but depicting MAS spectral albedo.

Figure 6 illustrates a times series of MAS reflectances and albedos for two 500 m × 500 m areas located on and near Lake Mendota (see **Figure 2** for locations). Snowfall and snowdepth recorded at the Madison airport for period from January 25 to February 15, 1997 are also given. Over the study period, the area experienced several snowfalls of over 2 inches (January 26th, February 4th, 10-12th, and 14th) and significant melting from February 1st through 3rd. Consequently, changes in the albedos of the lake and urban areas should be detectable from the MAS imagery. Given the large changes in the surface reflectances during the 17-day period as measured by the MAS, a single representative albedo could not be derived nor would a single value capture the temporal variability in surface albedo caused by synoptic meteorological events.

While MAS imagery was acquired on 7 of the 17 days during the study period, spectral albedos (represented by triangles) could be determined for only four of the days due to several compounding factors. On January 30th, persistent cloud cover obscured the region, On February 6th, solar zenith angles were in excess of 78°, making the atmospheric correction questionable, and hence no spectral albedo was calculated. The most interesting MAS acquisition occurred on February 2nd. At this time no snow was recorded at the airport and as can be seen in **Figure 6**, the uncorrected and atmospherically corrected reflectances are low for both the two areas shown in **Figure 2.** This is consistent with the meteorological observations that indicate zero snow depth at

the airport for February 2nd and 3rd. Field observations also indicate that on this day, the mean snow grain size had increased to 1200-1750 μm and the upper 1 to 2 cm of the snowpack was actively melting.

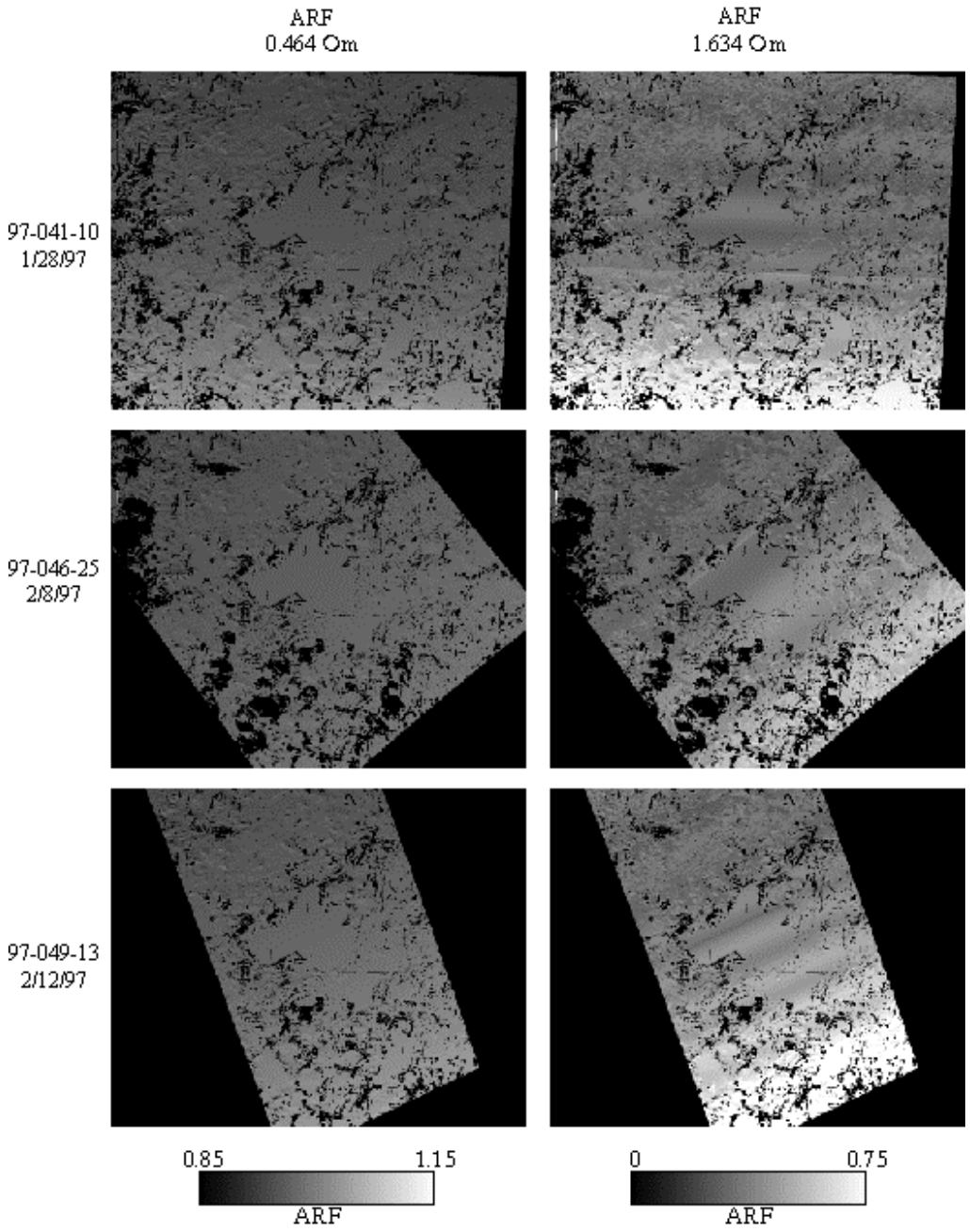

Figure 5. Anisotropic Reflectance Factor (ARF) images for three MAS scenes at 0.464 μm (left) and 1.634 μm (right). Note the larger variations in ARF over the scenes at the longer wavelength.

Both the meteorological and field observations suggest that snow albedo should be lower on February 2nd than on other days during the WINCE campaign. Unfortunately, a spectral albedo was not calculated for this date because the MODIS cloud mask had mapped the area as cloud-covered. The erroneous cloud cover determination appears to be caused by the thermal bands used by the cloud mask. Even if the cloud mask had determined the area to be cloud-free, the solar

zenith angle at the time of image collection was 70°, which is at the upper limit of acceptability for atmospheric correction.

However, the limited MAS timeseries highlights two important factors. First, cloud cover and the high solar zenith angles present at high latitudes during winter will make it necessary to attempt to determine snow albedo on a daily basis. Second, frequent MODIS snow albedo determinations are required to characterize the temporal changes in albedo during snow accumulation and ablation periods. This is especially true during the spring and fall. At these times the sun higher in the sky than during midwinter and the solar radiation contributes significantly to energy balance of a snowpack. Also, compared to midwinter when snow cover is extensive and significant melting has not yet started the albedo of a snowpack during spring and fall is far more variable.

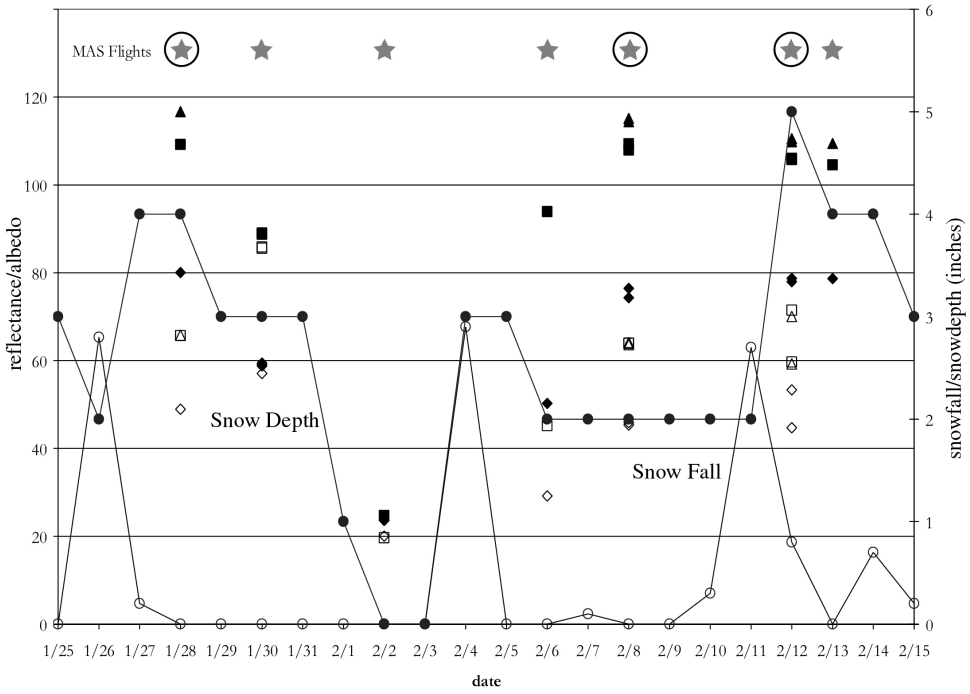

Figure 6. Time series of MAS band 2 (0.546 μm) reflectances and spectral albedos for two 500 x 500 meter sites located on Lake Mendota (solid symbols) and adjacent land (open symbols). Uncorrected (diamond), atmospherically corrected (square) and MAS spectral albedo (triangle) retrievals are plotted for each MAS image. Snow fall and snow depth are also shown. Stars highlight the dates of MAS flights and surrounding circles indicate the dates of the images shown in Figures 2 and 3.

CONCLUSIONS

A large body of research has paved the way for the development of a prototype snow albedo algorithm for use with NASA's recently launched MODIS instrument. A prototype algorithm was developed and tested on MAS images acquired over Wisconsin and New York during January and February of 1997. The developed prototype algorithm follows the work of (Fily *et al.*, 1997; Stroeve *et al.*, 1997) using a discrete ordinate radiative transfer model to model the bidirectional reflectance of a snow covered surface. The modeled BRDF is used to correct for anisotropic scattering effects over land covers that are dominated by snow while a simple Lambertian assumption is retained for snow-covered forests.

Despite the limitations of the MAS and the lack of concurrent field observations for validation, the overall performance of the prototype albedo algorithm is encouraging and the algorithm's performance will undoubtedly improve with the availability of MODIS data. The two largest

unresolved issues in developing an operational version of the algorithm are (1) the development of a narrow-to-broadband conversion to covert the MODIS spectral reflectances into broadband albedo estimates and (2) correction for anisotropic scattering effects in the shortwave infrared region of the spectrum. These problems are currently being addressed as the prototype algorithm is being adapted for use with data from the MODIS instrument.

ACKNOWLEDGEMENTS

This work was supported by NASA contract NAG5-8137 and NAG5-9455. Melyssa Guerry provided valuable assistance. Dr. Nolin's work on this project was supported by NASA grant NAG5-6462.

REFERENCES

Ackerman, S. *et al.*, 1997. Discriminating clear-sky from cloud with MODIS. Algorithm Theoretical Basis Document (MOD35), http://modis.gsfc.nasa.gov/MODIS/ATBD/atbd_mod06.pdf: 124pp.

Barbieri, R. *et al.*, 1997. Draft of the MODIS Level 1B Algorithm Theortical Basis Document Version 2.0. Algorithm Theortical Basis Document (MOD01), http://eospso.gsfc.nasa.gov/ftp_ATBD/REVIEW/MODIS/ATBD-MOD-01/atbd-mod-01.pdf: 68 pp.

Barnett, T.P., Dumenil, L., Schlese, W., Roeckner, E. and Latif, M., 1989. The effect of Eurasian snow cover on regional and global climate variations. Journal of the Atmospheric Sciences, 46: 661-685.

De Abreau, R.A., Key, J., Maslanik, J.A., Serreze, M.C. and LeDrew, E.F., 1994. Comparison of in situ and AVHRR-derived broadband albedo over Arctic sea ice. Arctic, 147(3): 288-297.

DOI and USGS, 1986. Land Use Land Cover Digital Data from 1:250,000 and 1:100,000-Scale Maps Data User Guide 4, U.S. Geological Survey, Reston, VA.

Dozier, J. and Marks, D., 1987. Snow mapping and classification from Landsat Thematic Mapper. Annals of Glaciology, 9: 97-103.

Fily, M., Bourdelles, B., Dedieu, J.P. and Sergent, C., 1997. Comparison of *In Situ* and Landsat Thematic Mapper derived snow grain characteristics in the Alps. Remote Sensing of Environment, 59: 452-460.

Greuell, W. and de Wildt, M.D., 1999. Anisotropic reflection by melting glacier ice: Measurements and parameterizations in Landsat TM bands 2 and 4. Remote Sensing of Environment, 70(3): 265-277.

Gumley, L., Hubanks, P. and Masuoka, E., 1994. MODIS Airborne Simulator Level-1B Users Guide. http://ltpwww.gsfc.nasa.gov/MODIS/MAS/masdug.html.

Hall, D.K., Chang, A.T.C., Foster, J.L., Benson, C.S. and Kovalick, W.M., 1989. Comparison of In Situ and Landsat derived reflectance of Alaskan glaciers. Remote Sensing of Environment, 28: 23-31.

Hall, D.K., Foster, J.L., Salomonson, V.V., Klein, A.G. and Chien, J.Y.L., in press. Development of a technique to assess snow-cover mapping accuracy from space. IEEE Transactions on Geoscience and Remote Sensing.

Hall, D.K., Riggs, G., A. and Salomonson, V.V., 1995. Development of methods for mapping global snow cover using moderate resolution imaging spectroradiometer data. Remote Sensing of Environment, 54: 127-140.

Hall, D.K. *et al.*, 1998. Algorithm Theoretical Basis Document (ATBD) for the MODIS snow-, lake ice- and sea ice-maping algorithms, http://eospso.gsfc.nasa.gov/ftp_ATBD/REVIEW/MODIS/ATBD-MOD-10/atbd-mod-10.pdf., 50pp.

King, M.D. *et al.*, 1996. Airborne scanning spectrometer for remote sensing of cloud, aerosol, water vapor, and surface properties. Journal of Atmospheric and Oceanic Technology, 13: 777-794.

Klein, A.G. and Hall, D.K., 1999. Snow albedo determination using the NASA MODIS Instrument. In: S. Taylor and J. Hardy (Editors), Proceedings of the 56th Annual Eastern Snow Conference, Fredericton, New Brunswick, pp. 77-85.

Klein, A.G., Hall, D.K. and Riggs, G., 1998. Improving snow-cover mapping in forests through the use of a canopy reflectance model. Hydrological Processes, 12: 1723-1744.

Knap, W.H., Brock, B.W., Oerlemans, J. and Willis, I.C., 1999. Comparison of Landsat TM-derived and ground-based albedos of Haut Glacier d'Arolla, Switzerland. International Journal of Remote Sensing, 20(17): 3293-3310.

Knap, W.H. and Oerlemans, J., 1996. The surface albedo of the Greenland ice sheet: satellite-derived and in situ measurements in the Søndre Strømfjord area during the 1991 melt season. Journal of Glaciology, 42(141): 364-374.

Leshkevich, G.A., Deering, D.W., Eck, T.F. and Ahmad, S.P., 1990. Diurnal patterns of the bi-directional reflectance of fresh-water ice. Annals of Glaciology, 14: 153-157.

Liang, S., Strahler, A. and Walthall, C., 1998. Retrievial of Land Surface Albedo from Satellite Observations: A Simulation Study, Geoscience and Remote Sensing Symposium (IGARSS '98), pp. 1286-1288.

Lindsey, R.W. and Rothrock, D.A., 1994. Arctic sea ice albedo from AVHRR. Journal of Climate, 7(11): 1737-1749.

Lucht, W., Schaaf, C.B. and Strahler, A.H., 2000. An algorithm for the retrieval of albedo from space using semiempirical BRDF models. IEEE Transactions on Geoscience and Remote Sensing, 38(2): 977-998.

Nicodemus, F.E., Hsia, F.C., Richmond, J.J., Ginsberg, I.W. and Limperis, T., 1977. Geometrical considerations and nomenclature for reflectance. Technical Report Monograph, 160. National Bureau of Standards, Gaithersburg, MD.

Nolin, A.W. and Liang, S., in press. Progress in bidirectional reflectance modeling and applications for surface particulate media: snow and soils. Remote Sensing Reviews.

Nolin, A.W. and Stroeve, J., 1997. The changing albedo of the Greenland Ice Sheet: implications for climate change. Annals of Glaciology, 25: 51-57.

Nolin, A.W. and Stroeve, J.C., 1999. Snow albedo determination and validation for MODIS and MISR, Proceedings of the Second International Workshop on Multiangular Measurements and Models, Ispra, Italy, p. 41.

O'Neill, A.D.J. and Gray, D.M., 1973. Spatial and temporal variations of the albedo of a prairie snowpack, The Role of Snow and Ice in Hydrology: Proceedings of the Banff Symposium. Unesco/WMO/IAHS, Geneva-Budapest-Paris, pp. 176-186.

Proy, C., Tanré, D. and Deschamps, P.Y., 1989. Evaluation of topographic effects in remotely sensed data. Remote Sensing of Environment, 30: 21-32.

Reijmer, C.H., Knap, W.H. and Oerlemans, J., 1999. The surface albedo of the Vatnajokull ice cap, Iceland: A comparison between satellite-derived and ground-based measurements. Boundary-Layer Meteorology, 92(1): 125-144.

Riggs, G.A., Hall, D.K. and Ackerman, S.A., 1999. Sea ice extent and classification with the Moderate Resolution Imaging Spectroradiometer Airborne Simulator (MAS). Remote Sensing of Environment, 68(2): 152-163.

Robinson, D.A. and Kukla, G., 1985. Maximum surface albedo of seasonally snow-covered lands in the Northern Hemisphere. Journal of Climate and Applied Meteorology, 24: 402-411.

Stamnes, K., Tsay, S., Wiscombe, W. and Jayaweera, K., 1988. Numerically stable algorithm for discrete-ordinate-method radiative transfer in multiple scattering and emitting layered media. Applied Optics, 23: 2502-2509.

Steffen, K., 1987. Bidirectional reflectance of snow at 500-600 nm, Large Scale Effects of Seasonal Snow Cover (Proceedings of the Vancouver Symposium, August 1987). IAHS, pp. 415-425.

Steffen, K., 1996. Effect of solar zenith angle on snow anisotropic reflectance. In: Smith and Stamnes (Editors), IRS'96: Current Problems in Atmospheric Radiation, pp. 41-44.

Strahler, A. *et al.*, 1999. MODIS land cover product. Algorithm Theoretical Basis Document (ATBD) Version 5.0, http://modis.gsfc.nasa.gov/MODIS/ATBD/atbd_mod12.pdf.

Stroeve, J., Nolin, A. and Steffen, K., 1997. Comparison of AVHRR-derived and in situ surface albedo over the Greenland Ice Sheet. Remote Sensing of Environment, 62: 262-276.

Taylor, V.R. and Stowe, L.L., 1984. Reflectance characteristics of uniform Earth and cloud surfaces derived from NIMBUS-7 ERB. Journal of Geophysical Research, 89(D4): 4987-4996.

Vermote, E.F., Tanré, D., Deuze, J.L., Herman, M. and Morcrette, J.J., 1997. Second simulation of the satellite signal in the solar spectrum: an overview. IEEE Transactions on Geoscience and Remote Sensing, 35(3): 675-686.

Vermote, E.F. and Vermeulen, A., 1999. Atmospheric correction algorithm: spectral reflectances (MOD09). Algorithm Theoretical Basis Document, 107 pp.

Wanner, W. *et al.*, 1997. Global retrieval of bidirectional reflectance and albedo over land from EOS MODIS and MISR data: theory and algorithm. Journal of Geophysical Research, 102(D14): 17,143-17,161.

Winther, J-G., 1993a. Landsat TM derived and in situ summer reflectance of glaciers in Svalbard. Polar Research, 12(1): 37-55.

Winther, J-G., 1993b. Short- and long-term variability of snow albedo. Nordic Hydrology, 24: 199-211.